Available online at www.sciencedirect.com
SCIENCE DIRECT®
Current Applied Physics 3 (2003) 473–476
Current Applied Physics
Physics, Chemistry and Materials Science
www.elsevier.com/locate/cap

Formation of metallic $NbSe_2$ nanotubes and nanofibers

T. Tsuneta [a,*], T. Toshima [a], K. Inagaki [a], T. Shibayama [a], S. Tanda [a], S. Uji [b], M. Ahlskog [c], P. Hakonen [c], M. Paalanen [c]

[a] *Department of Applied Physics, Hokkaido University, Sapporo 060-8628, Japan*
[b] *National Institute for Materials Science, Tsukuba, Ibaraki 305-0003, Japan*
[c] *Low Temperature Laboratory, Helsinki University of Technology, Espoo, Finland*

Received 28 April 2003; received in revised form 17 June 2003; accepted 14 July 2003

Abstract

We succeed in synthesizing $NbSe_2$ nanotubes along with nanofibers by chemical vapor transportation. They are stable crystalline systems and can be synthesized reproducibly in a nearly equilibrium reacting process. We have investigated these nanosize structures of $NbSe_2$ by transmission electron microscopy and electron diffraction. Both of the structures have a similar size of 100–200 nm in diameter. While nanotubes consist of rolled-up $NbSe_2$ layers, nanofibers are a pile of thin flat layers. We propose a mechanism of the formation of $NbSe_2$ nanotubes and nanofibers on the basis of deseleniditive transition from a $NbSe_3$ fiber-shaped crystal. We also measured electrical resistance of the nanofibers with conductive atomic force microscopy and demonstrated that the material show metallic behavior at room temperature.

PACS: 81.07.De; 73.63.Fg; 81.10.Jt
Keywords: Nanotube; Formation mechanism; Superconductor; Charge-density-wave

1. Introduction

The discoveries of fullerenes [1], carbon nanotubes (CNT's) [2], and Möbius crystals [3] as topological forms of matter have opened a challenging field covering over solid state physics, chemistry and materials science with wide spectra of possible applications. Topological effects, like the Berry phase [4,5], originating from system geometry have attracted much attention both theoretically and experimentally.

On the other hand, CNT is regarded as a prospective replacement of traditional semiconductor-based devices for constructing integrated circuits because of its characteristic size of nanometers. The nanometer-scale size of CNT offers not only faster operation and lower power consumption of a circuit, but also nontraditional mesoscopic devices, for instance single electron transistors. A superconducting or charge-density-wave (CDW) nanotube creates possibilities for device design for nanotube circuits. However, the nanoscale regime has not been studied for superconductor and CDW conductor systems, in particular, many aspects of nanoscale CDW dynamics are still unknown [6]. Moreover, the interplay between topological effects and downsized effects of these collective quantum phenomena (CDW and superconductor) are imperious themes because of their connection to the fundamental understanding of quantum mechanics as well as the potential for device construction.

To investigate these effects, we have chosen $NbSe_2$ for constructing tubular nanostructure. Möbius crystal of $NbSe_3$ have been the only other topological material of CDW compound so far. While $NbSe_3$ has a one-dimensional chain structure, which makes it possible to form a Möbius ring, $NbSe_2$ have a graphite-like layered structure, which is responsible for the formation of topological materials such like CNT's. $NbSe_2$ exhibits CDW transition at 33 K, and becomes superconductor below 7.2 K. These properties make the matter a promising candidate of a superconducting and/or CDW nanotube [7], both of which will be a valuable member to the known nanotube family: a normal metal or a

* Corresponding author.
E-mail address: tsuneta@eng.hokudai.ac.jp (T. Tsuneta).
URL: http://exp-ap.eng.hokudai.ac.jp.

1567-1739/$ - see front matter © 2003 Elsevier B.V. All rights reserved.
doi:10.1016/j.cap.2003.07.002

semiconductor (carbon nanotubes), and insulators (BN [8], MoS_2 [9] and WS_2 [10] nanotubes). However, $NbSe_2$ nanotubes were so far merely produced under electron irradiation with extremely high energy [11], while nanotubes of MoS_2 and WS_2, whose crystal structures are similar to $NbSe_2$, were synthesized by various chemical methods. In this study, we present evidence of $NbSe_2$ multi-wall nanotubes with diameters of 30–200 nm formed by a nearly equilibrium chemical reaction in a controllable way. Also, we propose a formation mechanism of the $NbSe_2$ nanotube based on transition from a $NbSe_3$ nanofiber.

2. Experimental procedures

We abstracted nanosize objects from $NbSe_2$ powder synthesized by direct chemical vapor transportation (CVT) method through following procedures. We put high-purity niobium (4N) and selenium (4N) in evacuated (10^{-6} Torr) silica ampoules as initial materials. The ampoules are then heated to the maximum temperature of 800 °C by a rate of 10 °C/min inside a furnace that has a spatial gradient of 1 °C/cm. Note that this method can be applied to synthesize niobium selenides with different composition, such as $NbSe_3$, by setting appropriate reaction temperature. After an hour of reaction, the ampoules are quenched to room temperature. Obtained $NbSe_2$ powder is suspended in dichloroethane or isopropyl alcohol by sonication of few minutes, and then nanosize particles in the dispersion are deposited on a substrate.

3. Results and discussions

3.1. Nanotubes and nanofibers

Fig. 1(a) shows a transmission electron microscope (TEM) image of a $NbSe_2$ nanotube found in deposition. The 200 nm wide, 1.3 μm long material sticking out of a bulk crystal shows an internal structure. The insets show enlarged views of internal structure from respective parts of the fiber. A transmission electron diffraction (TED) pattern (Fig. 1(b)) of the material has a 2 mm symmetry, and is composed of the spots aligned in rows vertical to the fiber. The crystal structure derived from the pattern is that of a hexagonal with $a/c = 0.27$, agreeing with that of 2H–$NbSe_2$ (hexagonal, $a/c = 0.274$, $a = 3.444$ Å and $c = 12.552$ Å). Nevertheless the material is not any other niobium-selenides including fiber-shaped compounds $NbSe_3$, Nb_2Se_3, etc. The diffraction spots can be indexed as shown in Fig. 1(b). The unindexed ones are diffractions by a tiny affix.

The material has clear features of a tubular structure in its TED pattern as follows. In the pattern, each hexagonal ($hk0$) spot accompanies diffraction spots with nonzero c^*-component, (hkn) ($n = 1, 2, 3\ldots$), aligned horizontally and outwardly. This aspect is crucial to a tubular structure according to the previous studies on CNT [12]. Hence the structure shown in Fig. 1 is an internal cavity of a width of 60 nm. We estimate the number of layers of the material as 120, which is too much to obtain an atomic image. Also we should point out that all coaxial shells of the tube have the chirality of armchair, i.e. a $\langle 1\,0\,0\rangle$ direction is toward the longitudinal axis.

We discovered another kind of nanofibers formed along with $NbSe_2$ tubes. Fig. 2(a) shows typical lattice image of a fiber without any cavity. The shown lattice spacing of 6.44 Å corresponds to interlayer distance of $NbSe_2$ (6.276 Å). It means that the micrograph depicts the side-surface of a $NbSe_2$ nanofiber consisting of stacked ribbon-shaped crystal layers. The same structure is verified by a TED pattern (Fig. 2(b)) of another fiber containing only ($hk0$) diffractions. The longitudinal axis of most nanofibers is also along a $\langle 1\,0\,0\rangle$ axis, as in Fig. 2(b).

We believe that the origin of our $NbSe_2$ nanotubes is scrolling of nanofibers. Actually, we once observed a

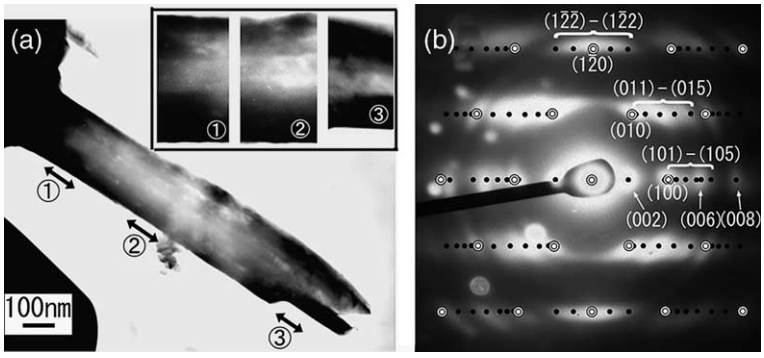

Fig. 1. (a) A TEM micrograph of a 200 nm wide, 1.3 μm long open-end nanotube sticking out of a bulk crystal. An internal cavity of 60 nm in width is shown in insets, which are enlarged views of respective parts of the material. (b) Each ($hk0$) diffractions in this TED pattern of the $NbSe_2$ nanotube is accompanied by (hkn) ($n = 1, 2, 3\ldots$) diffractions aligned in an array perpendicular to the longitudinal axis of the material. This aspect is characteristic of a tubular structure.

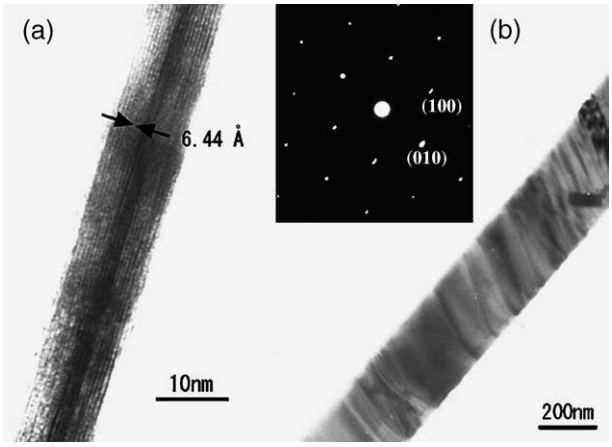

Fig. 2. (a) This TEM image of a nanofiber shows lattice spacing of 6.44Å that agree with (0 0 2) plane of 2H–$NbSe_2$. (b) A TEM image of another $NbSe_2$ nanofiber, whose TED pattern (inset) shows only one set of hexagonal diffractions. Both of the materials are ribbon-shaped $NbSe_2$ nanofibers having the a–b plane as its facet.

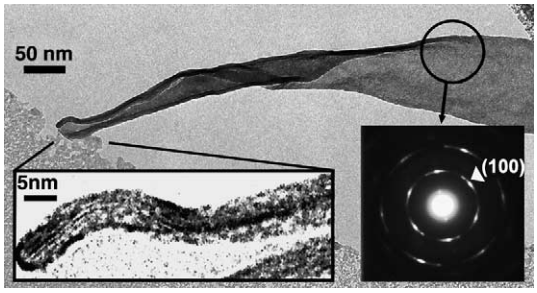

Fig. 3. A TEM micrograph of a part of a 110 nm wide, 2 μm long $NbSe_2$ nanofiber that began folding under an electron irradiation. The left end was made into a scroll (left inset). Its TED pattern (right inset) agrees with the a^*–b^* plane of $NbSe_2$.

fiber irradiated by an electron beam began scrolling and eventually formed a tube-like structure. Here we present a TEM image of the "intermediate" structure between nanotubes and ribbon-shaped nanofibers (Fig. 3). The right part of the 110 nm wide, 2 μm long fiber has the shape of a thin ribbon. Its TED pattern (right inset) indicates a hexagonal pattern with $d_{100} = 2.97$ Å, and agrees with the a^*–b^* plane of $NbSe_2$. However, the rest of the material is folded and the end of the fiber is almost completely scrolled, just like scroll-type CNT's [13].

3.2. Formation model

Next, we present a model of nanotube formation via intermediate nanofiber (Fig. 4 shows a schematic). Usually a fiber-shaped crystal of $NbSe_2$ cannot be formed by an equilibrium growth, because the largest facet should have six-fold rotation symmetry. However, we found the possibility of the transition from a $NbSe_3$ fiber into a $NbSe_2$ fiber by deselenidation. $NbSe_3$ has a chain-like structure along the b-axis and always makes a fiber-shaped crystal. A deseleniditive transition from $NbSe_3$ chains to a $NbSe_2$ layer would be achieved through union of an array of parallel chains into a plane (the configuration of Nb atoms along a chain is kept unchanged) because the Nb–Nb distance along a $NbSe_3$ chain (3.478 Å) is very close to that within a $NbSe_2$ plane (3.444 Å) and the intra-chain bonding is strong compared to the inter-chain bonding. As a result, a $NbSe_3$ fiber made of parallel chains becomes a $NbSe_2$ fiber made of stacked strips.

This model is consistent with experimental results. We observed that the a-axis of most $NbSe_2$ fibers is along the longitudinal direction. This fact agrees with the atomic configuration of our model, in which the a-axis of $NbSe_2$, the direction of Nb–Nb bonds, replaces the b-axis of $NbSe_3$ that is along the length of a fiber as well as Nb–Nb bonds. Although we supposed presence of $NbSe_3$ in first place, it is reasonable that $NbSe_3$ are synthesized first during heating process, because temperature reaches the optimum reaction temperature for $NbSe_3$ (740 °C) earlier than that for $NbSe_2$ (800 °C).

In expansion of this model, the deselenidation can also cause curvature to a $NbSe_2$ fiber. The deselenidation would propagate from the surface to inner layers. In the transient stage of the propagation, a few $NbSe_2$ layers cling to surface of $NbSe_3$. On this occasion, discord between Nb–Nb distance within a $NbSe_2$ layer and that across $NbSe_3$ chains eventuate in a stress that makes $NbSe_2$ layers scrolled lengthwise (see Fig. 4(d) for an illustration). A similar mechanism is known for kaolinite minerals [14] that have a cylindrical structure originated from discord in in-plane atomic distance between adjacent layers.

3.3. Electric properties

Preliminary studies on electric properties of the $NbSe_2$ nanofibers were performed in room temperature. Standard electron beam (e-beam) lithography and focused ion beam (FIB) deposition techniques were used to fabricate electrodes on the fibers. By e-beam lithography, four fingers of gold film with adhesive layer of titanium were deposited on the fibers. However, we have not succeeded by e-beam lithography to make electrical conduction between the electrode and the sample to date. This is probably due to a thin insulating layer on the surface of the fibers because we could make a good contact by FIB deposition of tungsten with high acceleration voltage. Since there is a crucial disadvantage of the FIB-deposited tungsten due to its superconducting

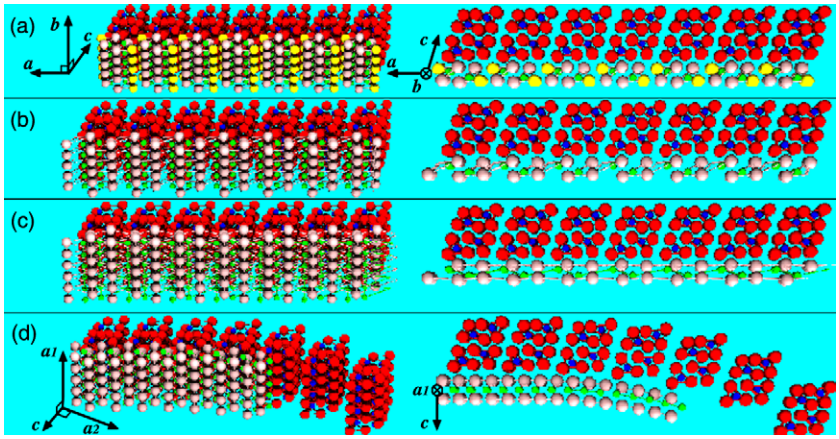

Fig. 4. Our model of deselenidative transition from a $NbSe_3$ fiber to a $NbSe_2$ nanotube. The outermost layer, which we suppose to transit into $NbSe_2$ first, is colored differently. (a) A $NbSe_3$ fiber composed of one-dimensional molecular chains along the *b*-axis. The yellow Se atoms are to be removed by deselenidation. (b) The voids produce inter-chain attraction. (c) The chains unite into a two-dimensional layer of $NbSe_2$. (d) Because of discord between inter-chain distance of $NbSe_3$ and in-plane atomic distance of $NbSe_2$, the $NbSe_2$ layer at surface shrinks dragging the inner $NbSe_3$ layers. Consequently, a scrolling $NbSe_2$ nanofiber is formed.

nature, e-beam lithography should be developed for low-temperature measurement. From the measurement of the FIB deposited fiber, in-plane resistivity was calculated as 7×10^{-7} Ω m.

In addition to these methods for making electrodes, we used the tip of the AFM as an electrode directly placed on the sample. The conductive tip is made of silicon single crystal with platinum coat. The $NbSe_2$ fibers were deposited on an indium film of a thickness of 200 nm. The performance of this system was tested with multiwall CNT's, and confirmed that the resistances were in agreement with literature values. By applying the load of 200 nN at the AFM tip end to penetrate the surface insulating layer, a current of 5×10^{-9} A flowed at 1×10^{-3} V bias, corresponding to the resistance of 200 kΩ. A crude estimation of the resistivity ranges 10^{-3}–10^{-2} Ω m. This value is relatively in good agreement with that perpendicular to the *c*-axis, 4×10^{-5} Ω m.

4. Summary

We have presented evidence of the formation of $NbSe_2$ nanotubes and nanofibers by chemical vapor transportation method. And we have proposed a model of the formation of nanotubes and nanofibers via transition from a $NbSe_3$ nanofiber. Also, we confirmed metallic conductivity of the nanostructures in room temperature.

It is an important problem whether the $NbSe_2$ nanotube can be a superconductor, because superconductivity is affected by topology of the system. Electron beam holography with cryogenic system will reveal nature of the electron properties of such the "topological materials".

Acknowledgements

The authors are grateful to K. Yamaya, Y. Okajima, N. Hatakenaka and M. Hayashi. We also acknowledge S. Iijima and K. Suenaga for useful discussions, and H. Takahashi and K. Sugawara for providing experimental apparatus. This work is supported by Grant-in-Aid for Scientific Research (B), Grant-in-Aid for Exploratory Research, and Grant-in-Aid for Encouragement of Young Scientists of the Ministry of Education, Culture, Sports, Science and Technology in Japan.

References

[1] H.W. Kroto, J.R. Heath, S.C. Obrien, R.F. Curl, R.E. Smalley, Nature 318 (1985) 162.
[2] S. Iijima, Nature 354 (1991) 56.
[3] S. Tanda, T. Tsuneta, Y. Okajima, K. Inagaki, K. Yamaya, N. Hatakenaka, Nature 417 (2002) 397.
[4] M.V. Berry, Proc. R. Soc. Lond. A 392 (1984) 45.
[5] T. Ando, T. Nakanishi, R. Saito, J. Phys. Soc. Jpn. 67 (1998) 2857.
[6] H.S.J. van der Zant, E. Slot, S.V. Zaitsev-Zotov, S.N. Artemenko, Phys. Rev. Lett. 87 (2001) 126401.
[7] G. Seifert, H. Terrones, M. Terrones, T. Frauenheim, Solid State Commun. 115 (2000) 635.
[8] A. Loiseau, F. Williame, N. Demoncy, N. Schramchenko, G. Hug, C. Colliex, H. Pascard, Carbon 36 (1998) 743.
[9] M. Remskar, Z. Skraba, F. Cléton, R. Sanjinés, F. Lévy, Appl. Phys. Lett. 69 (1996) 351.
[10] R. Tenne, L. Margulis, M. Genut, G. Hodes, Nature 360 (1992) 444.
[11] D.H. Galván, J.H. Kim, M.B. Maple, E. Adam, Fullerene Sci. Technol. 8 (2000) 143.
[12] S. Amelinckx, A. Lucas, P. Lambin, Rep. Prog. Phys. 62 (1999) 1471.
[13] S. Amelinckx, D. Bernaerts, X.B. Zhang, J. Van Tendeloo, J. Van Landuyt, Science 267 (1995) 1334.
[14] Hyde, Phys. Chem. Miner. 20 (1993) 190.